Analysis of Ga grading in CIGS absorbers with different Cu content

Analysis of Ga grading in CIGS absorbers with different Cu content

G. Sozzi[1], S. Di Napoli[1], R. Menozzi[1], R. Carron[2], E. Avancini[2], B. Bissig[2], S. Buecheler[2], A. N. Tiwari[2]

[1] Department of Information Engineering - University of Parma
Parco Area delle Scienze 181A, 43124 Parma, Italy

[2] Laboratory for Thin Films and Photovoltaics, Empa - Swiss Federal Laboratories for Materials Science and Technology, Ueberlandstrasse 129, CH-8600 Duebendorf, Switzerland.

***Abstract* - This work investigates the effect of Cu content and Ga grading on the performance of CIGS cells, by means of numerical simulations and comparison with corresponding experiments. Different Ga profiles and Cu average concentrations are considered. We show that the optical effect of Cu content must be properly taken into account to model NIR absorption. As far as the GGI profile is concerned, we show that the main improvement can be obtained by increasing the GGI ratio toward the back-side; an optimized notch bandgap profile can be designed with the help of these indications.**

***Index Terms* — Bandgap grading, CGI, CIGS, GGI, thin-film photovoltaics.**

I. Introduction

Intentional grading of the $Cu(In,Ga)Se_2$ (CIGS) absorber is commonly used in high efficiency solar cells [1]. Due to the dependence of CIGS bandgap on the [Ga]/([Ga]+[In]) ratio (GGI), increasing the Ga content widens the bandgap, mainly by up-shifting the conduction band edge [2]. In principle, optimized bandgap grading offers a better trade-off than constant-bandgap between V_{OC} (higher bandgap) and J_{SC} (lower bandgap), together with the possibility of improving carrier collection by means of the embedded grading-related electric field [3]. The so called "notch" or "double grading" profile has minimum bandgap at some distance into the CIGS layer and larger bandgap towards both back and front contacts. Lower bandgap at the absorber surface can also be designed to induce a type inversion at the CdS/CIGS interface. Solar cells at the state of the art exploit this bandgap grading idea, so a detailed understanding of its effects is useful. Moreover, Cu content also affects the cell performance [4]: therefore, we believe it is of interest to study how the effect of the [Cu]/([In]+[Ga]) ratio (CGI) combines with the GGI grading, with the final aim of presenting guidelines for the design of bandgap grading of high-efficiency CIGS solar cells.

II. Methods

A. Experiments

Four samples with *average* [Cu]/([In]+[Ga]) (CGI*) ratios of 0.8, 0.85, 0.9, 0.93 as measured by x-ray fluorescence spectroscopy (XRF). The corresponding measured GGI profiles show the typical "notch" observed in absorbers grown by co-evaporation with a multi-stage process.

The measured performance parameters of the 4 cells, performed under the AM 1.5 spectrum at 25 °C, show that increasing CGI* adversely affects the fill factor, FF, and open circuit voltage, V_{OC}, while the short circuit current density, J_{SC}, increases by some 3% when CGI* changes from 0.80 to 0.85, then more gently decreases as CGI* is raised from 0.85 to 0.93. As a result, the efficiency is maximum (19%) for CGI* = 0.80 and 0.85, then decreases by some 1% absolute as CGI* is increased to 0.93. The measured EQEs reflect the effect on J_{SC}: the increased near infrared (NIR) response observed when CGI* moves from 0.80 to 0.85 tends to saturate for CGI* > 0.85.

B. Simulations

We simulated the cell using the Synopsys Sentaurus-Tcad suite [5]. Details about the cell structure and main simulation parameters are reported in Table I and in [6].

TABLE I
MATERIAL PARAMETERS USED IN THE SIMULATIONS.

Material	ZnO	ZnO(i)	CdS	CIGS
Thickness [μm]	0.2	0.08	0.03	2
Doping [cm^{-3}]	$4\cdot10^{20}$	$1\cdot10^{17}$	$2\cdot10^{16}$	$1\cdot10^{16}$
Eg [eV]	3.3	3.3	2.4	graded
$\varepsilon/\varepsilon_0$	9	9	9	10
Nc [cm^{-3}]	$2.3x10^{18}$	$2.3x10^{18}$	$6.8x10^{17}$	$2.3x10^{18}$
Nv [cm^{-3}]	$3.3x10^{19}$	$3.3x10^{19}$	$1.5x10^{19}$	$1.8x10^{19}$
μ_e/μ_h [$cm^2/(V\cdot s)$]	100/25	100/25	100/25	100/25
ΔEc [eV]	-	-0.2		0.3
Bulk traps				
Nt [cm^{-3}]	10^{16} (acc.)	10^{16} (acc.)	$3\cdot10^{15}$ (acc.)	$6.67\cdot10^{14}$ (don.)
σ_e/σ_h [cm^2]	$10^{-15}/10^{-12}$			

In order to gain better insight of the observed device behavior, we performed a simulation study of the effects of bandgap grading for different CGI* ratio.

The measured GGI profiles are loaded into the model of the solar cell to give the corresponding bandgap grading profiles based on an experimentally tested second-order formula [2]. The optical behavior is described by complex refractive indexes depending on both GGI and CGI* ratios and coming from the literature [7].

III. Results

A. Effects of CGI

The simulated EQEs are shown in Fig. 1. The simulated behavior of the EQE shows a NIR shift between CGI* = 0.80 and 0.85, due to a step change in the absorption coefficient, and little variation beyond. While measurements do not show such a shift but rather a slope change, measurements and simulations agree on the lack of significant change for CGI* > 0.85.

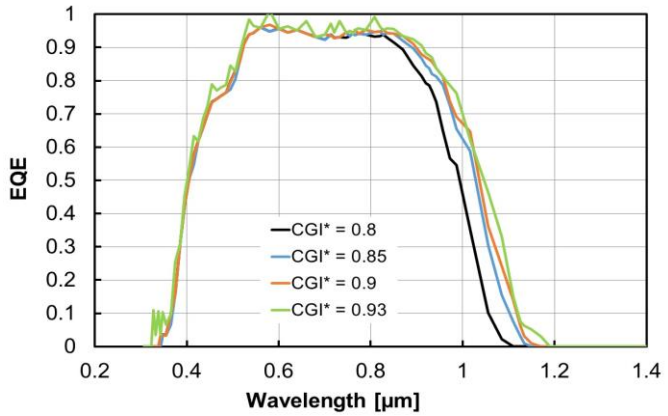

Fig. 1. Simulated external quantum efficiencies of the cells with different CGI* ratios and GGI grading.

A direct comparison between simulated and measured EQEs is shown in Fig. 2. No parameter fitting has been done. The simulations underestimate the cell's response at wavelength > 0.85 μm, especially for CGI* = 0.80.

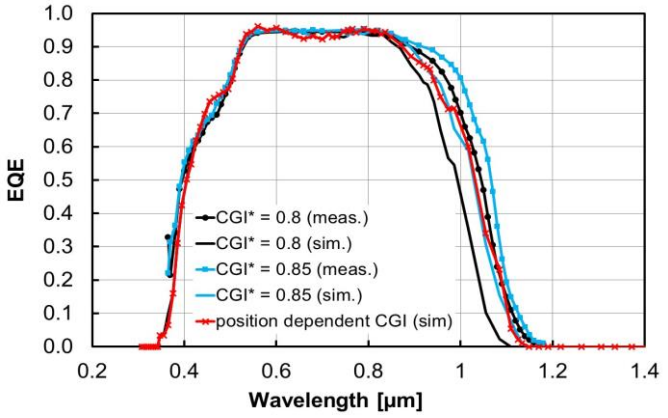

Fig. 2. Measured and simulated external quantum efficiencies for CGI* = 0.8 and 0.85. The red line is a simulation with average Cu content CGI* = 0.80 but non-uniform CGI.

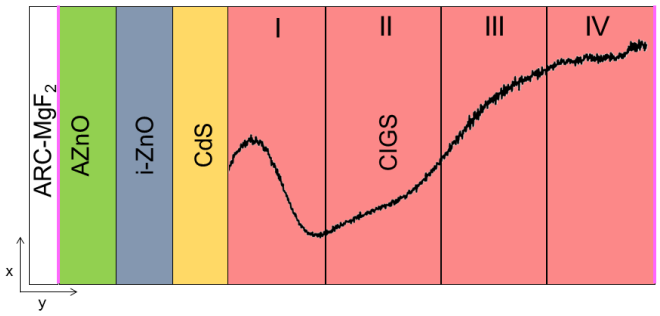

Fig. 3. A schematic representation of the simulated structure. The profile drawn across the CIGS is the GGI ratio. The CGI ratio is varied among regions I-IV as detailed in Table II.

However, it must be considered that in our simulations we are assuming uniform CGI = CGI* in the whole absorber, while in the real cell the CGI profile is not constant. To investigate this point, we simulated the structure shown in Fig. 3, where the CIGS is divided into four regions, and varied the CGI ratio as detailed in Table II.

TABLE II
SIMULATED STRUCTURE WITH NON-UNIFORM CGI

	Reg I CGI*	Reg II CGI*	Reg III CGI*	Reg IV CGI*
Case 1	0.7	0.7	0.7	**0.9**
Case 2	0.7	0.7	**0.9**	0.7
Case 3	0.7	**0.9**	0.7	0.7
Case 4	**0.9**	0.7	0.7	0.7

The simulated EQEs for the four cases of Table II, plotted in Fig. 4, show that the regions close to the front of CIGS and to the notch of the GGI profile (cases 3 and 4), determine the cell NIR absorption. Although the non uniformity of CGI displayed in Table II is purely speculative, Fig. 3 shows that assuming constant CGI* over the whole CIGS layer might be the reason of the gap between the measured and simulated EQEs in the NIR range when CGI* < 0.85 (black lines in Fig. 2).

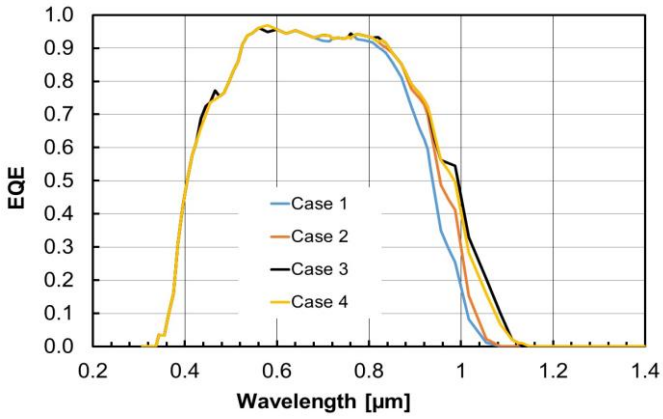

Fig. 4. Simulated external quantum efficiencies for different CGI profiles, as detailed in Fig. 3 and Table II.

Based on these results, we have simulated a cell with CGI* = 0.80 (average value), but non-uniform CGI (lower at the front and at the bottom, higher in the central part of the absorber): in this case, the simulated EQE (red line in Fig. 2) is very close to the measured one (black line with dots in Fig. 2) in the NIR range. In fact, absorption coefficients corresponding to an average CGI* < 0.85 will not adequately describe carrier generation in the CIGS regions where the non-uniform CGI is > 0.85, because of the step variation of the absorption coefficients described above.

More experimental and modeling activity will be required to clarify this point.

B. Effects of GGI

In order to study the sensitivity of cell parameters on the GGI grading profile, we considered the simplified model of notch grading shown in Fig. 5. Different bandgap profiles are simulated by varying the coordinates of points 0 (0, y_0), A (x_A, y_A), B (x_B, y_B), and C (3 µm, y_C), where x is the depth inside the CIGS layer and y is the corresponding GGI ratio. The optical coefficients used for CIGS in all the simulations correspond to a value of CGI* = 0.9, and vary consistently with GGI as given in [7].

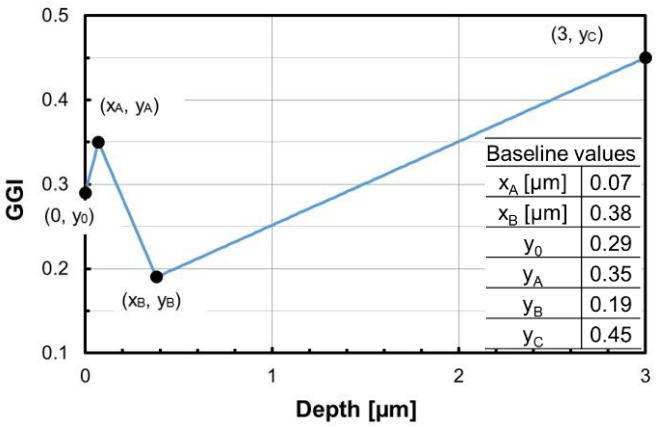

Fig. 5. Simulated [Ga]/([Ga]+[In]) (GGI) profile, for CGI* = 0.9. The coordinates y_0, x_A, y_A, x_B, y_B, y_C have been varied in the simulations. The inset reports the coordinates corresponding with the baseline profile.

We choose a baseline GGI profile (see the inset of Fig. 5) corresponding with η = 21.0%, J_{SC} = 34.4 mA/cm^2, V_{OC} = 0.745 V and FF = 81.9%. Only one of the coordinates is varied at a time, while the others are kept at their baseline value.

B1. Variation of x_A and x_B

Varying the depth of the GGI peak x_A (in the range 0.03 - 0.13 µm) and the depth of the notch x_B (in the range 0.14 - 0.32 µm,) has negligible effect on all the figures of merit, the relative changes observed being < 0.5%.

B2. Variation of y_0, y_A, y_B and y_C

The increase of the surface GGI y_0 mainly affects FF and η, which respectively earn almost 2% and 1% absolute, for y_0 varying from 0.20 to 0.38 (Fig. 6).

On the contrary, when the peak GGI y_A increases from 0.3 to 0.4, J_{SC} loses 1 mA/cm^2 and η decreases by almost 1% absolute, as shown in Fig. 7. Similarly, when the minimum GGI y_B is increased from 0.12 to 0.24, J_{SC} and η decrease (Fig. 8), while V_{OC} and FF improve (not shown).

In the case where we varied the back-side GGI y_C, a significant efficiency gain comes from the increase of V_{OC} (Fig. 9), while J_{SC} and FF are almost unchanged (not shown). However, for y_C > 0.55 the performance enhancement tends to saturate.

The analysis described so far shows that the increase of GGI at the molybdenum side of the CIGS absorber (y_C) is expected to give the best results.

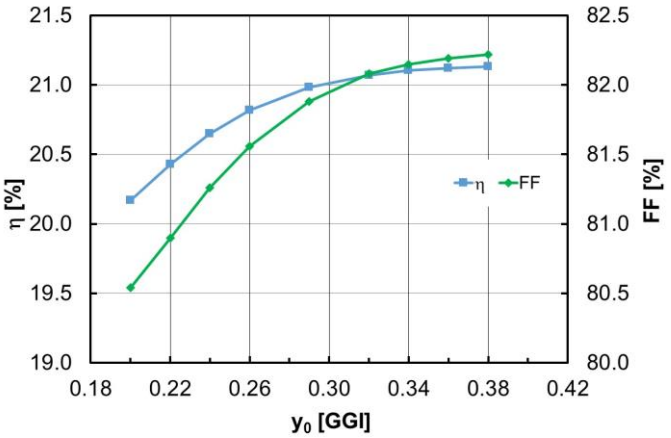

Fig. 6. Simulated η and FF versus y_0 (as defined in Fig. 5); other (baseline) parameter values in the inset of Fig. 5.

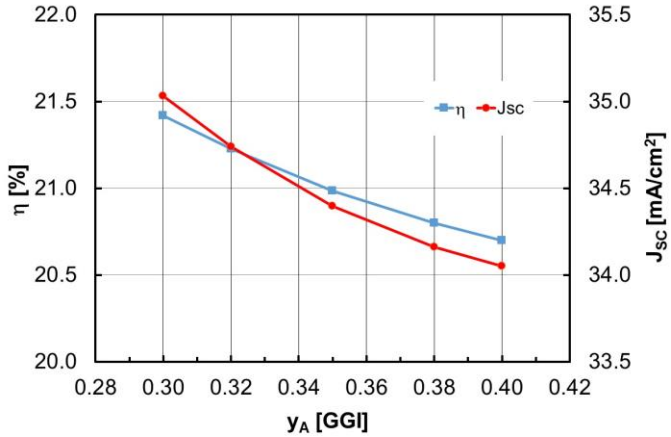

Fig. 7. Simulated η and J_{SC} versus y_A (as defined in Fig. 5); other (baseline) parameter values in the inset of Fig. 5.

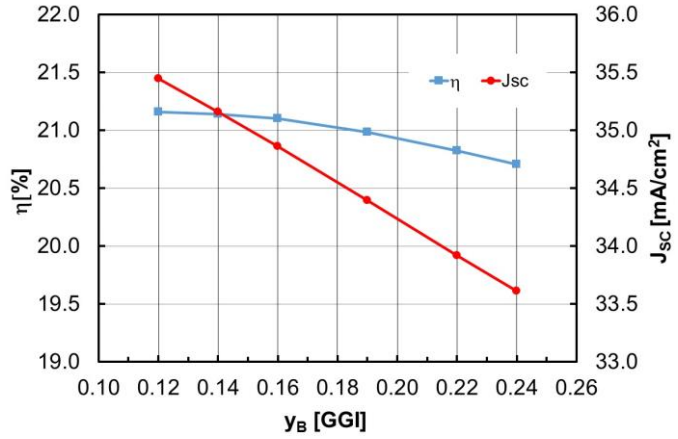

Fig. 8. Simulated η and J_{SC} versus y_B (as defined in Fig. 5); other (baseline) parameter values in the inset of Fig. 5.

If we consider the baseline back-side GGI ratio $y_C = 0.45$ and choose for the other coordinates the values giving the best performance in the simulations described above, we obtain: $V_{OC} = 0.737$ V, $J_{SC} = 35.8$ mA/cm^2, FF = 81.7% and $\eta = 21.6\%$. On the other hand, for $y_C = 0.6$ we get: $V_{OC} = 0.768$ V, $J_{SC} = 35.7$ mA/cm^2, FF = 81.1% and $\eta = 22.2\%$.

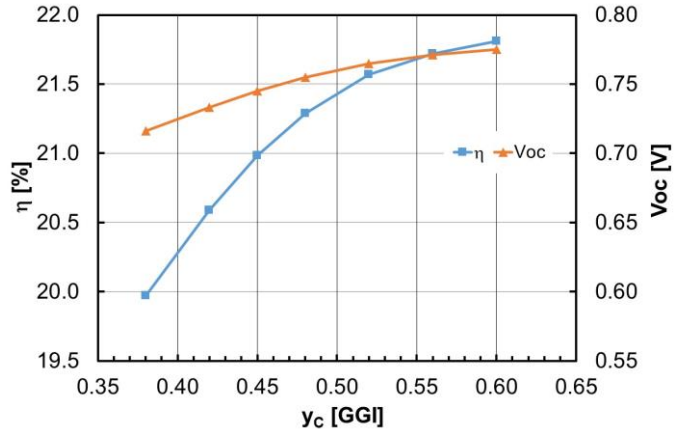

Fig. 9. Simulated η and V_{OC} versus y_C (as defined in Fig. 5); other (baseline) parameter values in the inset of Fig. 5.

VI. Conclusion

This work focuses on the use of numerical simulations to study how different CGI and GGI profiles affect the performance of CIGS cells. We show that: i) CGI must be properly taken into account to model the cell's absorption in the NIR range; ii) increasing the average CGI above 0.85 leads only to slight increment of Jsc, different values of average CGI > 0.85 giving very similar EQEs; iii) as far as the GGI profile is concerned, we show that the main improvement in cell performance can be obtained by increasing the GGI ratio toward the back-side; an optimized notch bandgap profile can be designed with the help of these indications.

Acknowledgement

This project has received funding from the *European Union's Horizon 2020 research and innovation programme* under grant agreement No 641004, project Sharc25.

References

[1] M. Powalla, P. Jackson, W. Witte, D. Hariskos, S.Paetel, C. Tschamber, W. Wischmann, "High-efficiency Cu(In,Ga)Se2 cells and modules", *Solar Energy Materials & Solar Cells,* vol. 119, pp. 51–58, 2013.

[2] S-H. Wei, S.B. Zhang and A. Zunger, "Effects of Ga addition to CuInSe2 on its electronic, structural, and defect properties", *Applied Physics Letters,* vol. 72, pp. 3199-3201, 1998

[3] J. Song, S.S. Li, C.H. Huang, O.D. Crisalle, T.J. Anderson, "Device modeling and simulation of the performance of $Cu(In_{1-x},Ga_x)Se_2$ solar cells", *Solid-State Electronics*, vol. 48, pp. 73–79, 2004.

[4] P. Jackson, D. Hariskos, R. Wuerz, W. Wischmann, and M. Powalla "Compositional investigation of potassium doped Cu (In,Ga)Se2 solar cells with efficiencies up to 20.8%", *Phys. Status Solidi RRL* 8, No. 3, pp. 219–222, 2014.

[5] http://www.synopsys.com/Tools/TCAD.

[6] G. Sozzi, D. Pignoloni, R. Menozzi, F. Pianezzi, P. Reinhard, B. Bissig, S. Buecheler, A. N. Tiwari, "Designing CIGS solar cells with front-side point contacts", *Proc. 42th IEEE Photovoltaic Specialists Conference (PVSC)*, 2015; doi: 10.1109/PVSC.2015.7355691.

[7] S. Minoura, T. Maekawa, K. Kodera, A. Nakane, S. Niki, and H. Fujiwara, "Optical constants of Cu(In, Ga)Se2 for arbitrary Cu and Ga compositions", *Journal of Applied Physics*, vol. 117, pp. 195703 - 195703-12, 2015.